RHYTHMIC ACTIVITY IN THE MEDIAL FRONTAL CORTEX ENCODES RELATIVE REWARD VALUE

Linda M. Amarante[1], Marcelo A. Caetano[2], and Mark Laubach[1*]

[1]Department of Biology and Center for Behavioral Neuroscience, American University, Washington, DC, USA; [2]Center for Mathematics, Computation and Cognition, Universidade Federal do ABC, Santo André, Brazil

*Corresponding author:
Mark Laubach, PhD
Department of Biology &
Center for Behavioral Neuroscience
Asbury 300
American University
4400 Massachusetts Avenue NW
Washington, DC 20016-8062
mark.laubach@american.edu

Abbreviated title: Value coding by the medial frontal cortex

Conflict of Interest: None

Financial Support: NSF grant 1121147, NIH grant DK099792-01A1, and the Klarman Family Foundation to ML and a NSF Graduate Research Fellowship to LMA.

Abstract

How do we know the reward value of a given food or fluid? The item must first be consumed and only then can its relative value be computed. Rodents consume fluids by emitting rhythmic trains of licks and reward value is likely encoded by neuronal activity entrained to the lick cycle. Here, we investigated the relationship between licking and reward signaling by the medial frontal cortex (MFC), a key cortical region for reward-guided learning and decision-making. Rats were tested in an incentive contrast procedure, in which they received alternating access to higher and lower value sucrose rewards. Neuronal activity in the MFC encoded the relative value of the ingested fluids, showing stronger entrainment to the lick cycle when animals ingested higher value rewards. The signals developed with experience, encoded the reward context, and depended on neuronal processing within the MFC. These findings suggest that consummatory behavior drives reward signaling in the MFC.

Introduction

The medial frontal cortex (MFC) is a crucial brain region for the adaptive control of behavior. Across species, the MFC monitors behavioral outcomes and enables adjustments in performance (Shidara and Richmond, 2002; Ito et al., 2003; Amiez et al., 2006; Narayanan and Laubach, 2006; Luk and Wallis, 2009; Sul et al., 2010; Narayanan et al., 2013). In behavioral neuroscience studies, information about behavioral outcomes must be generated by the act of consuming foods and fluids given as rewards for correct responding. However, interpretations of MFC processing have largely been drawn from experiments in which reward-related signaling was measured in responses to reward predictive stimuli (e.g. Otis et al., 2017) or during the period of reward consumption without regard to the animal's ongoing ingestive behavior (e.g. Jezzini et al., 2013; Donnelly et al., 2014).

A recent study from our laboratory (Horst and Laubach, 2013) reported that licking influences neural activity in the pregenual MFC. Neuronal firing rates were modulated around bouts of licks, which were further denoted by phase-locking of field potentials in the theta range (4-8 Hz). These signals might be expected given the anatomy of the pregenual MFC. The medial part of the pregenual MFC, called the prelimbic cortex (aka area 32), is reciprocally connected with the agranular insular cortex (Gabbott et al., 2003), which contains taste-responsive neurons (e.g. Stapleton et al., 2006). Moreover, the most prominent subcortical projections of the prelimbic cortex are to subcortical autonomic centers such as the hypothalamus, periaqueductal gray, and nucleus of the solitary tract (Floyd et al., 2000; Floyd et al., 2001; Gabbott et al., 2006; Reppucci and Petrovich, 2015). These connections may mediate the ability of the prelimbic cortex to regulate breathing (Hassan et al., 2013), which must be adjusted with regard to consummatory actions.

The more lateral part of the rostral MFC, called the medial agranular cortex (AGm or M2), has been described as "jaw opening" motor cortex (Yoshida et al., 2009; Haque et al., 2010) and projects to the trigeminal motor (Yoshida et al., 2009) and sensory (Iida et al., 2010) nuclei. A number of studies have recently examined the caudal (peri-callosal) part of this region, and

established that it controls head movements (Erlich et al., 2011), whisking (Brecht et al., 2004), and action-based value selection (Kargo et al., 2007; Sul et al., 2011). This caudal part of the MFC may play a general role in adaptive choice behavior, specifically in mapping or integrating sensory signals into motor outputs (Barthas and Kwan, 2017). No study has examined the functional properties of the more rostral MFC, where Horst and Laubach (2013) reported prominent licking-related neuronal activity, with regard to reward-guided decisions.

Therefore, the goal of the present study was to address the role of the rostral MFC (prelimbic and AGm areas) in the control of reward-guided behavior. We used a simple take-it-or-leave decision-making task, called the Shifting Values Licking Task (Parent et al., 2015a,b), to study reward signaling in relation to ongoing consummatory actions. Rats lick on a spout to receive liquid sucrose rewards and the relative value of the fluids alternates between a better and worse option every 30 sec. Rats learn to persistently lick for the better option and suppress licking when the worse option is available. They show incentive contrast effects when tested with only single levels of rewards (i.e. the duration of licking bouts is prolonged when rats lick for a higher value fluid when it is presented in alternation with a lower value fluid compared to when only the higher value fluid is available). Bilateral reversible inactivations of the rostral MFC impair performance in this task (Parent et al., 2015a): With MFC inactivated, rats fail to show incentive contrast effects and demonstrate temporally fragmented licking (i.e. the duration of licking bouts is reduced). Opposite effects were found when rats are tested with drugs that enhance neuronal excitability, such as the hunger hormone ghrelin (Parent et al., 2015b).

To examine how the rostral MFC encodes relative reward values and controls value-guided consumption, we recorded spike activity and local field potentials (LFPs) as rats performed the Shifting Values Licking Task. We analyzed neuronal activity in relation to the animals' ongoing licking behavior and as a function of the relative reward value of the ingested solutions. We found that neuronal activity in the MFC encoded the relative value of the ingested fluids, showing stronger entrainment to the lick cycle when animals ingested higher value rewards. In some of the rats, we recorded neuronal activity as the rats progressed through the

initial sessions of operant training, and found that these signals developed with experience. Next, we modified the task to include periods of non-reinforced licking, so we could determine if the signals reflected the receipt of reward (perhaps driven by sensory information from the taste system). Surprisingly, we found that the neuronal coding of relative value persisted throughout the periods when the higher and lower value fluids were available, suggesting that the signals encode the reward context. Finally, we used unilateral reversible inactivations (via muscimol) to determine if the reward signals depended on processing by neurons in the MFC. The unilateral reversible inactivations had minimal effects on licking behavior (compared to Parent et al., 2015a), but reduced the differential encoding of reward value for neuronal signals recorded in the opposite hemisphere. Together, our findings suggest that consummatory behavior drives signaling in the MFC that is used to compare the relative reward values of ingested foods and fluids.

Results

To investigate the role of the frontal cortex in reward-related consummatory behaviors, we assessed licking behavior in rats while performing simultaneous recordings in the rostral MFC. We trained rats in the shifting values licking task (Parent et al., 2015a), in which they licked at a drinking spout to receive 0.025 ml of a liquid sucrose reward (Figure 1A). The reward value of the fluid switched between higher (20% sucrose wt/vol) and lower (2 or 4%) levels every 30 seconds. After only three to five 30 minute sessions, rats show increased licking for the high-value reward relative to their licking for the lower value solution (Figure 1B; paired t-test between high-value and low-value licks: $t_{(8)} = 4.29$, $p < 0.005$).

Eleven rats were implanted with multi-electrode arrays in the rostral MFC. In four of the rats, a drug cannula was implanted in the opposite hemisphere using the same stereotaxic coordinates (Figure 1C). Figure 1D shows the placement of where each electrode terminated in the MFC (specifically, within the medial agranular and prelimbic cortices).

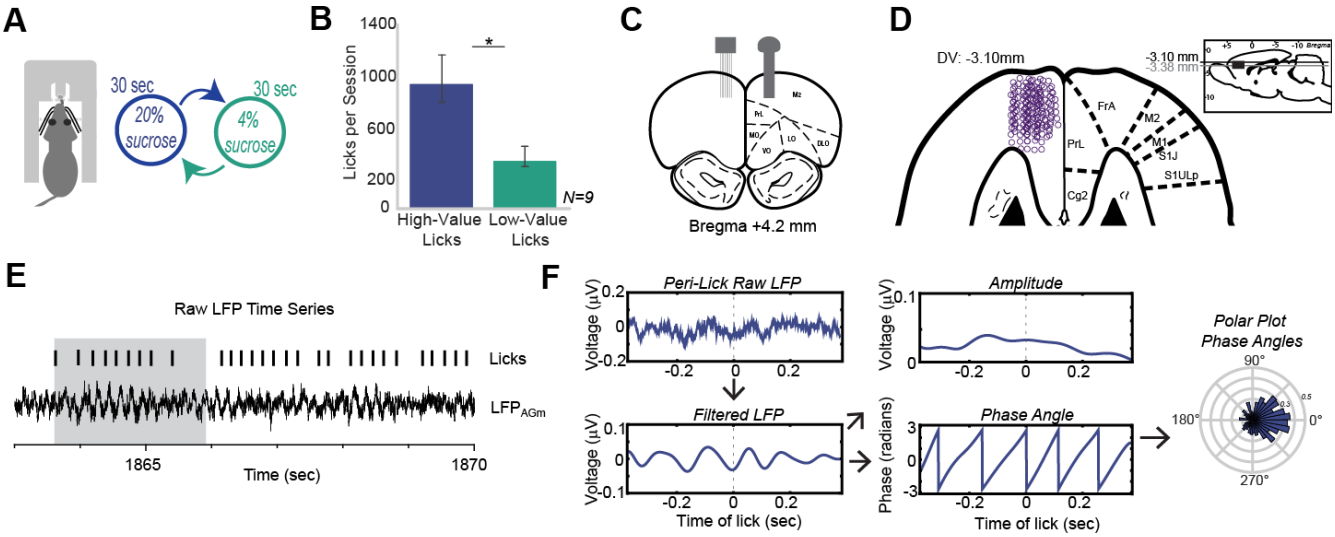

Figure 1: Behavioral task and neuronal recordings. *A. Rats were tested an incentive contrast procedure called the shifting values licking task (Parent et al., 2015a). They were required to lick on a spout to receive liquid sucrose rewards. Reward values shift between relatively high (20% wt/vol) and low (4% or 2% wt/vol) concentrations of sucrose every 30 seconds. B. Experienced rats (fourth training session) licked more for the high-value sucrose than for the low-value sucrose. Asterisk denotes p<0.005 (paired t-test; t(8) =4.29, p < 0.005). C. All 11 rats were implanted with a microwire array targeting the rostral medial frontal cortex (MFC) in one hemisphere and a subset of rats (N=4) had a drug cannula implanted in the opposite hemisphere. D. Locations of recording sites are depicted on a horizontal section from a standard rat atlas (Paxinos and Watson, 1997). E. An example of a local field potential (LFP) recording shows lick-entrained rhythmic activity. Gray box denotes delivery of fluid. F. Relationships between LFP signals and licking was assessed by bandpass filtering the LFPs around the licking frequency (defined by the inter-quartile range around the medial inter-lick interval) and applying the Hilbert transform to measure the amplitude and phase of licking-related neuronal activity. Instantaneous phase was measured, plotted using polar coordinates, and analyzed with standard methods for circular statistics (Agostinelli and Lund, 2013). See methods for details.*

Lick-entrained neuronal activity in the medial frontal cortex

We recorded local field potentials (LFP) from the MFC in rats as they ingested liquid sucrose in the shifting values licking task. Figure 1E shows a raw LFP trace from one electrode as one of the rats licked at the drinking spout for liquid sucrose. To measure entrainment between the LFPs and the animal's licking, we bandpass filtered the LFPs around the licking frequency and averaged the resulting peri-event data. This revealed rhythmic fluctuations in the LFPs synchronized to the lick cycle (Figure 1F, left panel). We then applied the Hilbert transform to the LFP signals, which allowed us to analyze the amplitude and phase of the LFPs (Figure 1F, middle

panel) and represent the phase of LFPs using circular histograms (also known as polar plots). These plots revealed tuning of the phase angles of the LFPs at the onset on licking (Figure 1F, right panel).

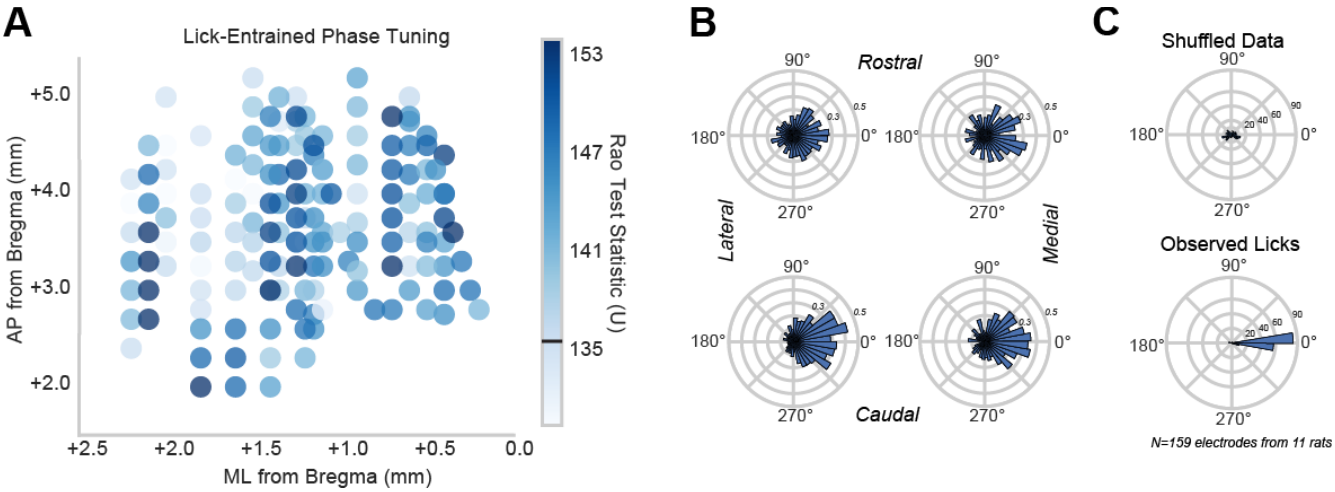

Figure 2: Neuronal activity in the MFC was entrained to the lick cycle. *A. Spatial plot of phase tuning using the test statistic from Rao's spacing test of uniformity. Individual electrode locations are plotted according to their location in reference to Bregma (N=159 electrodes). Recording sites are depicted as circles colored by the strength of their Rao test statistic (U). The colorbar shows values of U from the 5th to 95th percentile range over all recording sites. Values above the black bar (near 135) were not uniform (p<0.05). B. Polar plots represent phase tuning examples from four spatial extremes of the graph in (A). The most rostral/lateral (top left; U=134.48, p>0.05), rostral/medial (top right; U=152.30, p<0.001), caudal/medial (bottom right; U=153.51, p<0.001), and caudal/lateral (bottom left; U=147.44, p<0.001) electrodes were chosen. There was no drastic difference among the four locations with regard to phase tuning. C. Group summaries of the mean phase angle at the time of licking from all 11 rats reveal significant phase tuning toward 0 degrees (i.e. peak or trough of the rhythm). These results were compared with phase angles measured from surrogate data (shuffled inter-lick intervals), which did not show evidence for significant phase entrainment.*

To further investigate the relationship between licking and the phase angle of LFPs, we used circular statistics to measure the consistency of the phase angles at the time of licking from the LFPs (Figure 2). We used Rao's spacing test for uniformity, which assesses the directional spread of circular data. Each LFP was bandpass filtered near the licking frequency (±2 inter-lick intervals) and the Hilbert transform was used to measure the phase angles, as shown in the example in Figure 1F. We plotted each electrode's location in MFC and shaded them by the intensity of the test statistic from the Rao test (Figure 2A). The black horizontal line in the

colorbar on the right denotes a Rao test statistic that corresponds to a level for the Rao statistics at p=0.05. All shades above this line denote significant directional non-uniform tuning of the lick-entrained phase angles for that given electrode. Polar plots for four example electrodes (from four different rats) located in each extreme of MFC space (rostral/lateral, rostral/medial, caudal/lateral, and caudal/medial) are shown in Figure 2B. Remarkably, the electrodes had a mean phase angle near 0 degrees, i.e. at the peak or trough of the neural oscillation. While there was no anatomical specificity of phase tuning in MFC, the region as a whole showed a relatively similar phase that is suggestive of tuning to the lick cycle.

These results showing lick-entrained phase tuning of LFPs were significantly different from those obtained with surrogate data (based on shuffled inter-lick intervals). Figure 2C shows polar plots of the average angle from each electrode's lick-entrained LFPs (500 observed licks in the session) and from 500 randomly shuffled data points from the same session. Lick-entrained LFPs from each of the 11 rats in the study showed significant phase tuning towards the 0° direction, as opposed to 500 randomly sampled data points, which do not show any significant phase tuning in any direction. This suggests that LFP phase angles are tuned in a specific direction at the onset of licking, at the peak or trough of the neural oscillation.

While the polar plots revealed the phase angle at the onset on licking, it was still unclear of what frequency range the LFP's amplitude and phase were occurring. To do so, we used standard time-frequency analysis measures from human EEG research (eeglab toolbox in Matlab). We low-pass filtered the LFPs below 100 Hz and measured lick-related changes in spectral power (event-related spectral power or ERSP) and phase consistency at the times of the licks (inter-trial phase coherence or ITC). The ERSP analysis showed increased power below 10 Hz (Figure 3A, top row). We compared the results at lick-onset to randomly shuffled data that had the same time structure as the licks (shuffled data from inter-lick intervals, Figure 3 middle panel; see methods). Power at the lowest frequencies in the 2-4 Hz “delta” range) was also apparent in ERSP plots made with shuffled events, and was not evident in the difference plot (Figure 3, top right ERSP plot). This finding suggests that LFP power near the licking frequency

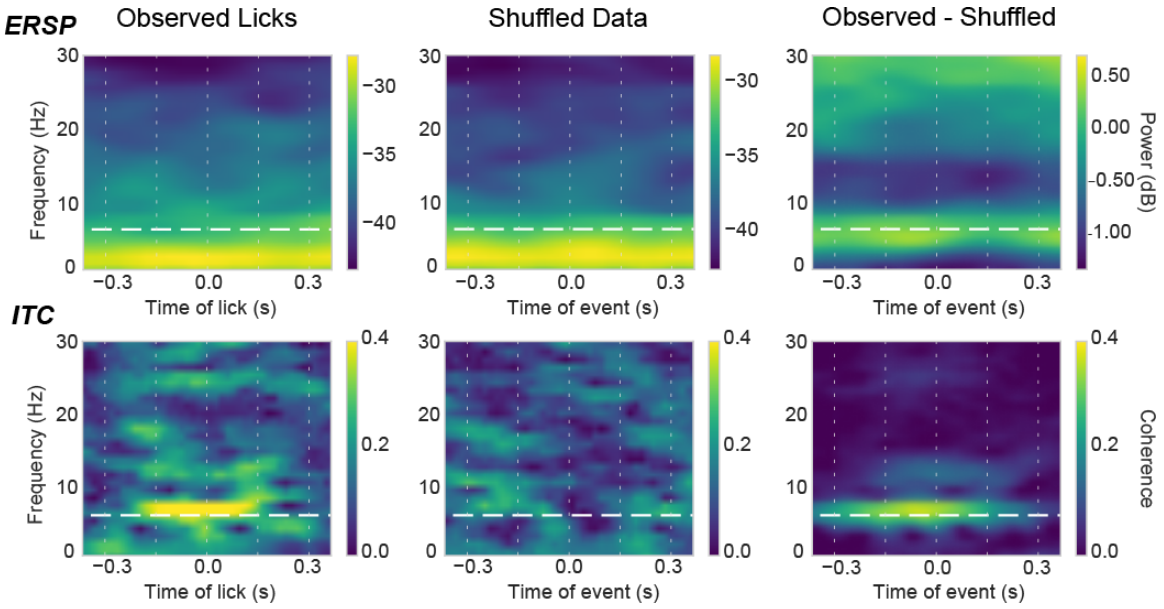

Figure 3: Time-frequency analysis of lick-entrained LFP data. *Event-Related Spectral Power [ERSP] (top) and Inter-Trial Coherence (ITC) are shown for a typical LFP recording aligned to the time of licking in the behavioral task. The white horizontal dashed line depicts the median licking frequency. The white vertical dashed lines depict the median inter-lick intervals. ERSP and ITC measures were computed using observed licks (left) and surrogate data (middle), created by shuffling inter-lick intervals. Persistent elevated ERSP was notable at very low frequencies (~2 Hz, or delta) for both the observed (upper left) and shuffled (upper middle) events, i.e. was not entrained to the lick cycle. Subtraction of the shuffled ERSP matrix from the observed ERSP matrix revealed elevated power at the licking frequency (horizontal dash line). ITC was apparent near the licking frequency over a period of two lick cycles for the observed licks (lower left), but not the shuffled licks ((lower middle). Subtraction of the shuffled ITC matrix from the observed ITC matrix revealed elevated power at the licking frequency (horizontal dash line).*

was phase-locked to the lick cycle. By contrast, delta power was not entrained to the lick cycle. We also found significant levels of ITC around the onset of licking (Figure 3, bottom row), specifically in the 6-8 Hz theta range. This level of phase-locking was significantly different from that obtained from the same analysis applied to LFPs at the times of randomly shuffled events (Figure 3, middle panel).

Rhythmic activity develops with experience and encodes reward value.

The previous results found lick-entrained neural activity in the MFC. The results in Figure 4 and in subsequent figures reveal within-session dynamics specifically associated with the rats experiencing two different concentrations of liquid sucrose. We chose to compare data from the

first and fourth training sessions based on a previous study from our lab showing asymptotic licking behavior by day 4 in the same task (Parent et al., 2015a). When trained in the shifting values licking task, rats quickly came to lick more for the high-value sucrose over days, and licked less for the low-value sucrose (Figure 4A). Median inter-lick intervals (ILIs) were reduced from session 1 to session 4 (Wilcoxon rank-sum test from three rats individually: $p<0.0001$), indicating that rats increased their licking frequency with experience in the task.

Repeated measures ANOVA found a main effect of reward value on licking ($F_{(1,14)}=32.20$, $p<0.001$). Tukey's posthoc test found evidence for a difference between the number of licks for the high-value versus low-value reward in session 4 ($p=0.013$), but not session 1 ($p=0.935$). Event-related potentials (ERPs) showed lick-entrained rhythmic activity in the fourth training session that was not apparent in the rats' first day of the training (Figure 4B). Notably, there was a distinction between high-value and low-value phase-locking to the onset of licking evident in LFP data from session 4, but this signal was not apparent during session 1. To capture effects of reward value on the LFPs, we calculated a "value index" for each electrode's ITC value index (Figure 4D, see methods) for sessions 1 and 4. (The value index was derived from difference between the high-value and low-value ITC values divided by the high-value ITC.) All electrodes from all rats showed an increase in the ITC value index, suggesting there was an increase in the difference between the phase-locking for high-value versus low-value licks by session 4 (paired t-test: $t(39)=-12.085$, $p<0.001$).

Additionally, ITC and ERSP spectral plots showed evidence for the development of lick-entrained phase-locking, specifically for the high-value licks, and a decrease in delta power for both types of licks, respectively (Figure 4C). While there were very low levels of phase-locking for high-value licks in session 1, a much stronger ITC developed by session 4 for the high-value licks. To measure changes in the signals associated with the two reward values over sessions, we performed a repeated-measures ANOVA with the maximum ITC values as the dependent variable and the values of the licks and the training sessions as predictors. This analysis found a significant interaction between session and value ($F_{(1,164)}=10.45$, $p<0.005$), and Tukey's posthoc

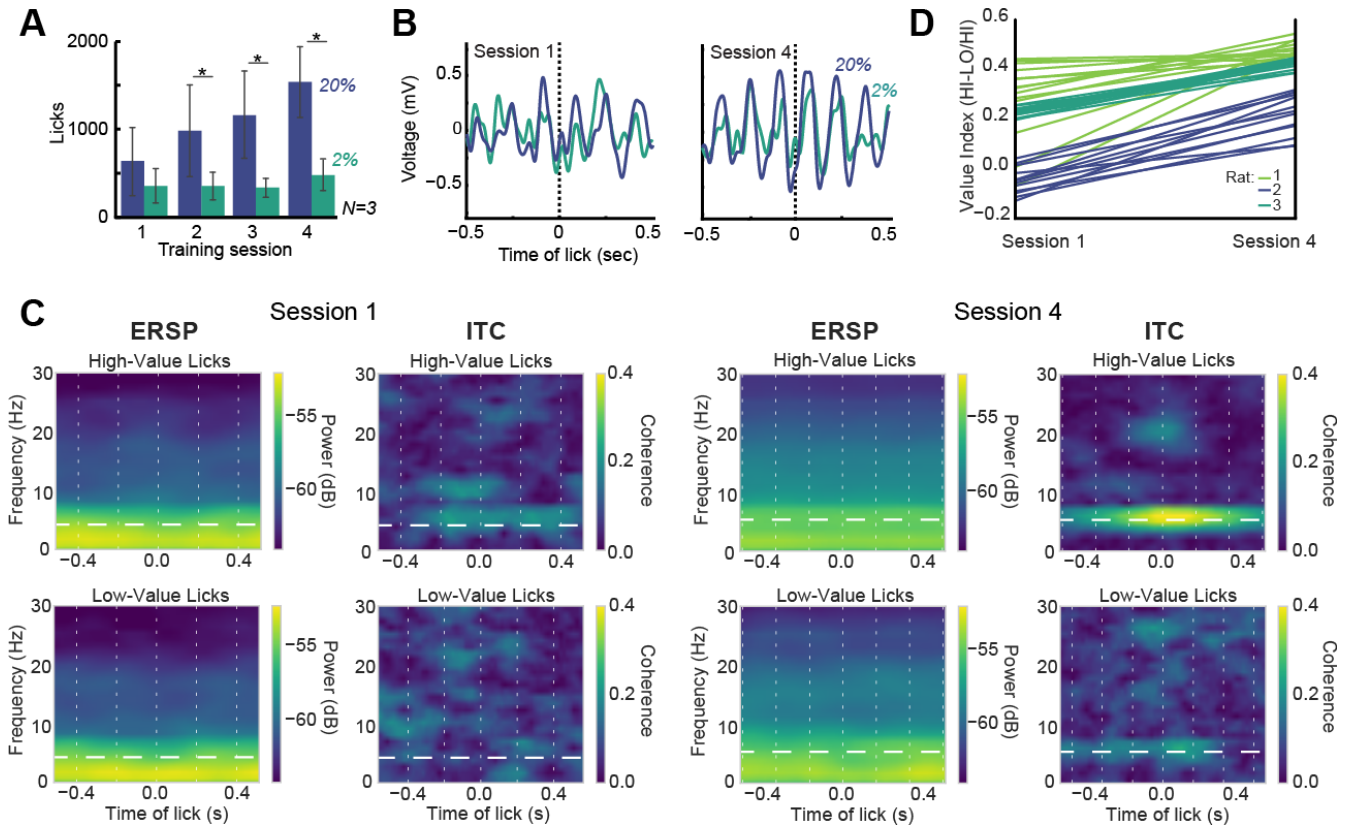

Figure 4: Rhythmic activity develops in MFC with experience and encodes reward value. *A. Recordings were made in a subset of three rats as they learned the behavioral task. The rats showed increased licking for the high-value sucrose compared to the low-value sucrose after the first training session and the relative difference in licking increased over the first four training sessions. Asterisk denotes p<0.05. B. Neuronal entrainment to the lick cycle developed with experience in the task. For example, Event-Related Potentials (ERP) increased in size and apparent rhythmicity between the first and fourth training session (blue = higher-value 20% sucrose; green = lower value 2% sucrose). C. Increased entrainment to the lick cycle was also apparent in Inter-Trial Coherence (ITC), which was not apparent in session 1 and specific to licks that delivered high-value sucrose in session 4. (White vertical lines = average inter-lick intervals across the session. White horizontal dashed line = average licking frequency across the session.) D. To capture differences in ITC values for the two types of licks across all recordings, we used a value index, defined as ITC-HI – ITC-LO)/ITC-HI. The index was based on the maximum ITC values in a temporal window ranging from one inter-lick interval before lick onset up to 50 ms after the lick and for all frequencies between 4 and 12 Hz ("theta"). As shown in the parallel line plot, in which each line denotes a LFP recording from a distinct electrode, this index was larger in session 4 compared to session 1 (paired t-test: t(39)=-12.085, p<0.001).*

test revealed differences between session 1 versus session 4 ITC values ($p<0.05$) and between high-value lick ITC and low-value lick ITC in session 4 ($p<0.001$). There was no difference

between high-value and low-value ITCs (p=0.14) in session 1. The difference in lick-entrained ITC strength that developed over days is evidence for an experience-dependent encoding of reward value by the rostral MFC.

We also assessed changes in LFP power by performing a repeated-measures ANOVA with the individual maximum ERSP values as the dependent variable and the value of the licks and training session as predictors, which revealed significant changes to the maximum ERSP values across sessions. There was a significant interaction between session and reward value ($F_{(1,163)}$=15.43, p<0.001). Tukey's post-hoc analyses showed a difference in power from session 1 to session 4 high-value licks (p<0.0001), as well as power for session 4 high and low value licks (p<0.0001), yet there was no difference in power between session 1 high-value and low-value licks (p=0.99). These findings suggest that both the power and phase of LFPs in the MFC are sensitive to experience in the licking task, and a distinction of both measures emerged over days, suggesting a role for the rostral MFC in encoding relative reward value.

Lick-entrained spike activity

While the previous results showed evidence for lick-entrained rhythmic activity and an encoding of reward value through LFPs in MFC, it was unclear if spike activity would show similar results. Spike recordings revealed strongly modulated activity synchronized to the lick cycle (Figure 5A). Multi-unit activity [MUA] (N=44, recorded from 3 rats in the 4th training session) was enhanced when rats licked for the high-value sucrose relative to the low-value sucrose (t(43)=3.78, p<0.001; Figures 5A and upper plot in 6A). The probability of spiking at the licks was below 0.3 for all multi-units, and was below 0.1 for instances when single units were isolated from the same recording sites. (For this reason, we focused on MUA in the present study.)

Neuronal entrainment to the lick cycle was measured using lick-spike coherence (using routines from Neurospec 2.0; see Methods). An example of lick-spike coherence for a unit that was selective to the higher value licks is shown in Figure 5B. Spectral power is shown for the licks (upper left plot) and spikes (upper right plot). The licks had a peak near the frequency

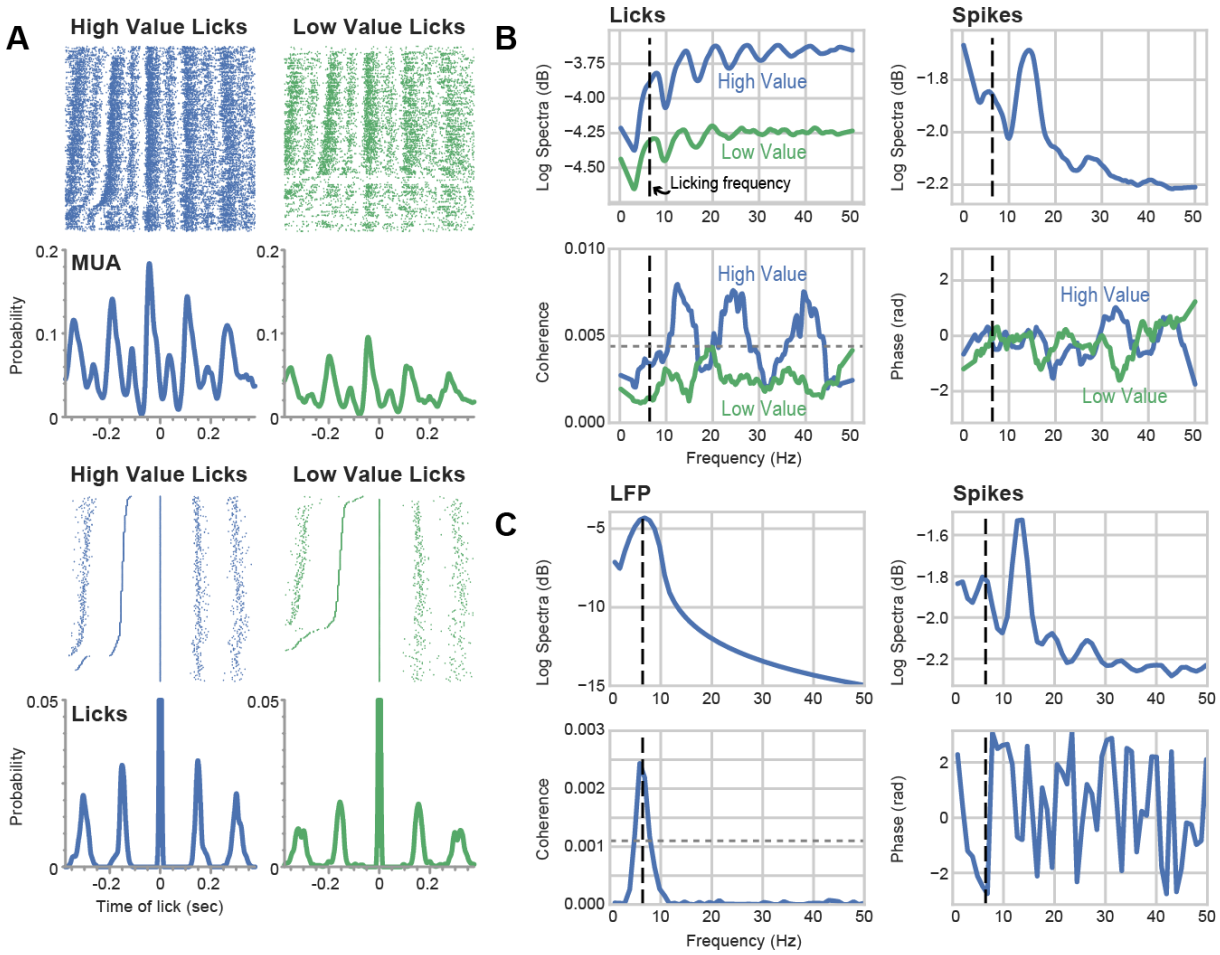

Figure 5: Spike activity in MFC was entrained to the lick cycle. *A. Example of multi-unit spike activity (top) and licks (bottom) entrained to the lick cycle when a rat consumed the higher (blue) and lower (green) value sucrose rewards. Raster plots show clear rhythmic spiking and licking. The rasters were sorted by the latency to the last lick before the lick at time 0, with the shortest preceding intervals at the top of the raster. The high value licks were sub-sampled for this plot so that neural activity and licking could be compared for the same number total licks (at time 0). Peri-event histograms (bin: 1 ms, 10-point Gaussian smoothing) denote the probability of spiking around the times of the licks. B. Example of spike-lick coherence (MUA from panel A). Spectral analysis of the licking point processes showed peaks at the licking frequency (black dashed line) and higher harmonics of that frequency (left). By contrast, the spike train had its largest spectral peak at ~15 Hz, in the low beta range. A smaller peak was also apparent at the licking frequency. Spike-lick coherence showed multiple peaks in the low beta (12-16 Hz Hz), high beta (22-27 Hz), and gamma (38-43 Hz) ranges for the high value licks. No peaks were above the 95% confidence interval (gray dashed line) for the low value licks. Phase was near 0 for these signals. C. Example of spike-field coherence. Spectral analysis of a bandpass filtered LFP (as in Figure 1) showed a single broad peak at the licking frequency. The spectral plot for the simultaneously recorded spike train is the same as in panel C. Spike-field coherence was apparent at the licking frequency (5.96 Hz), at a level approximately twice the 95% confidence interval. The phase between the spikes and fields was near –P at the licking frequency (lower right plot).*

defined by the median inter-lick interval (black dash line), and harmonics at higher intervals of that frequency. The blue and green traces depict the spectral power for the higher and lower value licks, respectively. The spikes had a major peak at ~14 Hz and minor peaks at the licking frequency and in the high beta and gamma ranges. Coherence values at frequencies up to 50 Hz are shown in the lower left plot in Figure 5B. The unit was not coherent with the licks at the licking frequency but had multiple significant peaks in the low (~14 Hz) and high (~25 Hz) beta and gamma (~40 Hz) ranges for the high value, but not the low value, licks. Phase was near zero at the licking frequency (lower right plot in Figure 5B). Over all units, 33 of 44 units (75%) fired in phase with licks that delivered the higher value fluid. Only 19 of these units (43%) fired in phase with licks that delivered the lower value fluid. Similar to the effect of relative value on spike probabilities, spike-lick coherence was greater for the higher value licks compared to the lower value licks (lower plot in Figure 6A; proportions test: Chi square = 7/9, df = 1, $p<0.01$).

Most of the units with significant spike-lick coherence showed peaks in the beta and gamma ranges, and there was no consistent frequency associated with lick-spike coherence (Figure 6B). (This might be expected given the multi-unit nature of the spike data.) There was no simple relationship between spike probability and spike-field coherence (upper plot in Figure 6C), except that units with low spike-lick coherence tended to have low spike probabilities.

Given the general lack of spike-lick coherence at the licking frequency, despite the common finding of beta and gamma coherence, we examined spike-field coherence using the same bandpass filtered LFPs used to analyze for lick-entrainment (Figure 1,2). This analysis revealed all 44 MUA recordings exhibited significant levels of spike-field coherence at frequencies associated with the licking cycle. An example of spike-field coherence is shown in Figure 4C. Similar to the phase measurements of the LFPs (Figure 2), spikes and fields tended to be in phase near the peak of the LFP rhythm (lower right plot in Figure 5D). Similar to spike-field coherence, there was no simple relationship between spike probability at the time of the licks and spike-field coherence (lower plot in Figure 6C). Overall, these analyses show clear relationships between spike activity, the lick cycle, and LFP fluctuations that encode relative

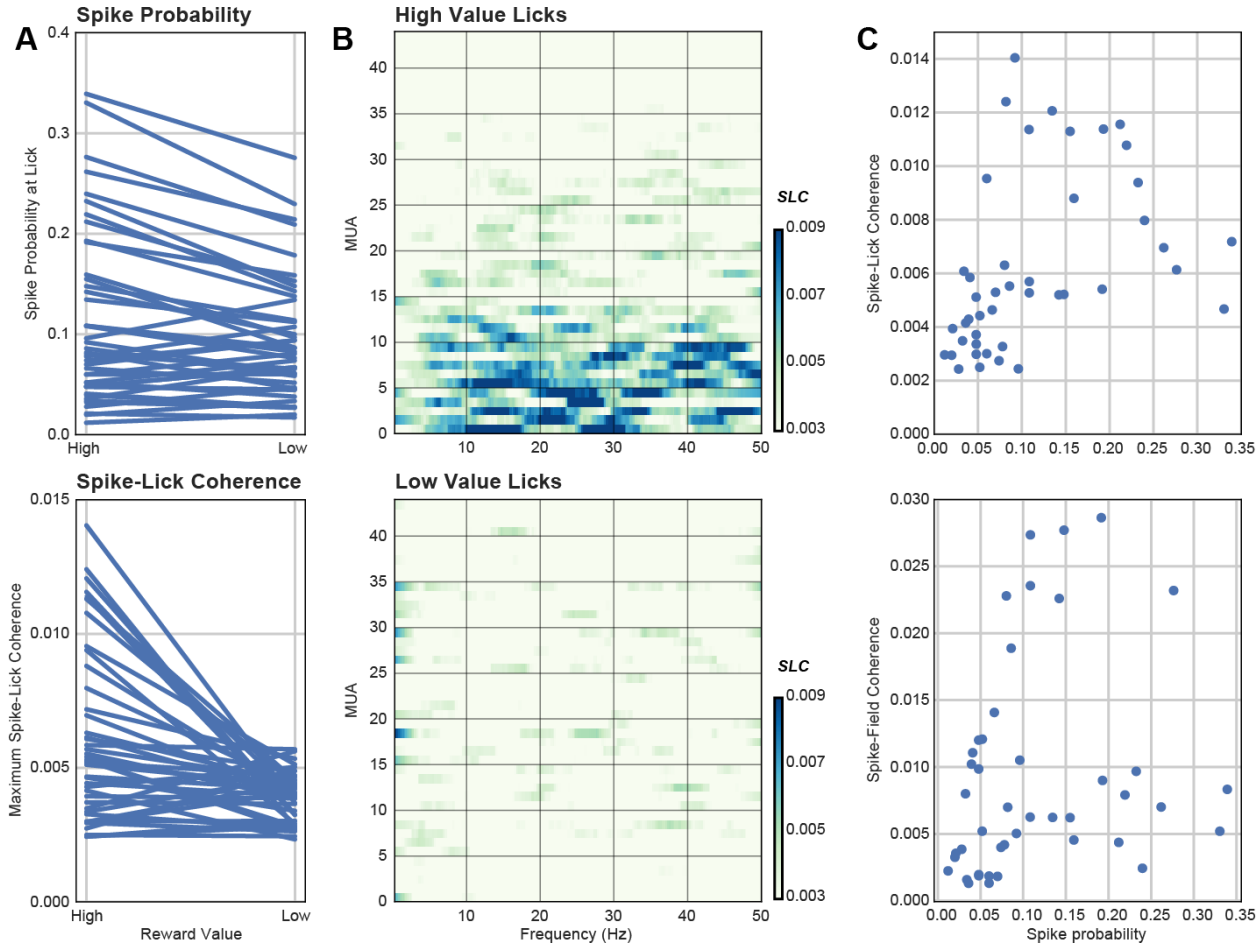

Figure 6: Spike activity in MFC encoded relative reward value. *A. Parallel line plot for spike probability and spike-lick coherence at times of higher and lower value licks. Each line denotes a recording of multi-unit activity. Both measures were greater for the higher value licks compared to the lower value licks over all recordings (spike probability: t(43)=3.78, p<0.001; spike-lick coherence: t(43)=4.60, p<0.001). B. Frequencies associated with spike-lick coherence (SLC) are shown in a matrix plot for coherence plotted as false color over the range of frequencies (2-50 Hz) for the 44 units. Results were complex, as no single frequency was associated with the relative difference in reward value. However, many units that fired in phase with licking were coherent at frequencies in the beta (10-30 Hz) and/or gamma ranges (>30 Hz). C. There was no simple relationship between spike probability (at the time of the licks) and spike-lick coherence (upper plot) or spike-field coherence (lower plot). That is, units with the highest likelihoods of spiking during the licks were not necessarily entrained to the lick cycle (SLC) or the ongoing LFP rhythms near the licking frequency (SFC).*

reward value. However, the relations between these variables were complex and could not be reduced to a single cortical rhythm linking the behavioral and neuronal measures.

Reward context, not reinforcement, drives licking-related theta entrainment

The signals described above could simply reflect an encoding of the taste properties of the ingested solutions by the rostral MFC. To examine this issue, we modified the shifting values licking task to include a 2 second period of non-reinforced licking between periods of fluid delivery (Figure 7A). This procedure resulted in rats continuously licking during the non-reinforced blocks of the task (Figure 7B). All rats continued to lick more during these non-reinforced blocks when they could receive the high-value fluid compared to when they could receive the low-value fluid ($t_{(5)}$ = 4.25, p<0.005 for all high-value context licks against all low-value context licks; $t_{(5)}$=4.87, p<0.005 for non-reinforced high-value context licks versus non-reinforced low-value context licks; $t_{(5)}$=-4.92, p<0.005 for reinforced high-value context licks versus reinforced low-value licks). Additionally, LFP signals synchronized to reinforced and non-reinforced licks were similar, with the main differences between high-value licks and low-value licks still evident despite the adjustment to the task. Figures 7C and D show group summaries of the differences in ERSP and ITC values at the onset of the reinforced and non-reinforced high-value licks. Of all electrodes from 6 rats trained in the adjusted task, there are minimal differences in ERSP values (Figure 7C). LFP activity also showed no major change in maximum ERSP between each lick value's reinforced versus non-reinforced licks ($F_{(1,359)}$=2.52, p>0.05 for interaction between lick type and reward type), which is evident in the spectral plots from one channel in an example rat in Figure 6E.

However, the majority (60 of 91) of the electrodes (from all rats) showed increases in phase-locking for the non-reinforced high-value licks (Figure 7D). We performed a repeated-measures ANOVA with factors for lick type (reinforced or non-reinforced) and reward value (high or low) with maximum ITC values as the dependent variable. This analysis found evidence for a significant interaction between lick type and reward value (F(1,359) = 31.94, p < 0.001). The non-reinforced licks had slightly greater ITC values at the onset of licking (high-value reinforced licks = 0.48, SD = 0.069; high-value non-reinforced licks = 0.51, SD = 0.063), which was also confirmed using Tukey's posthoc test (reinforced versus non-reinforced high-value licks, p<0.05). Spectral

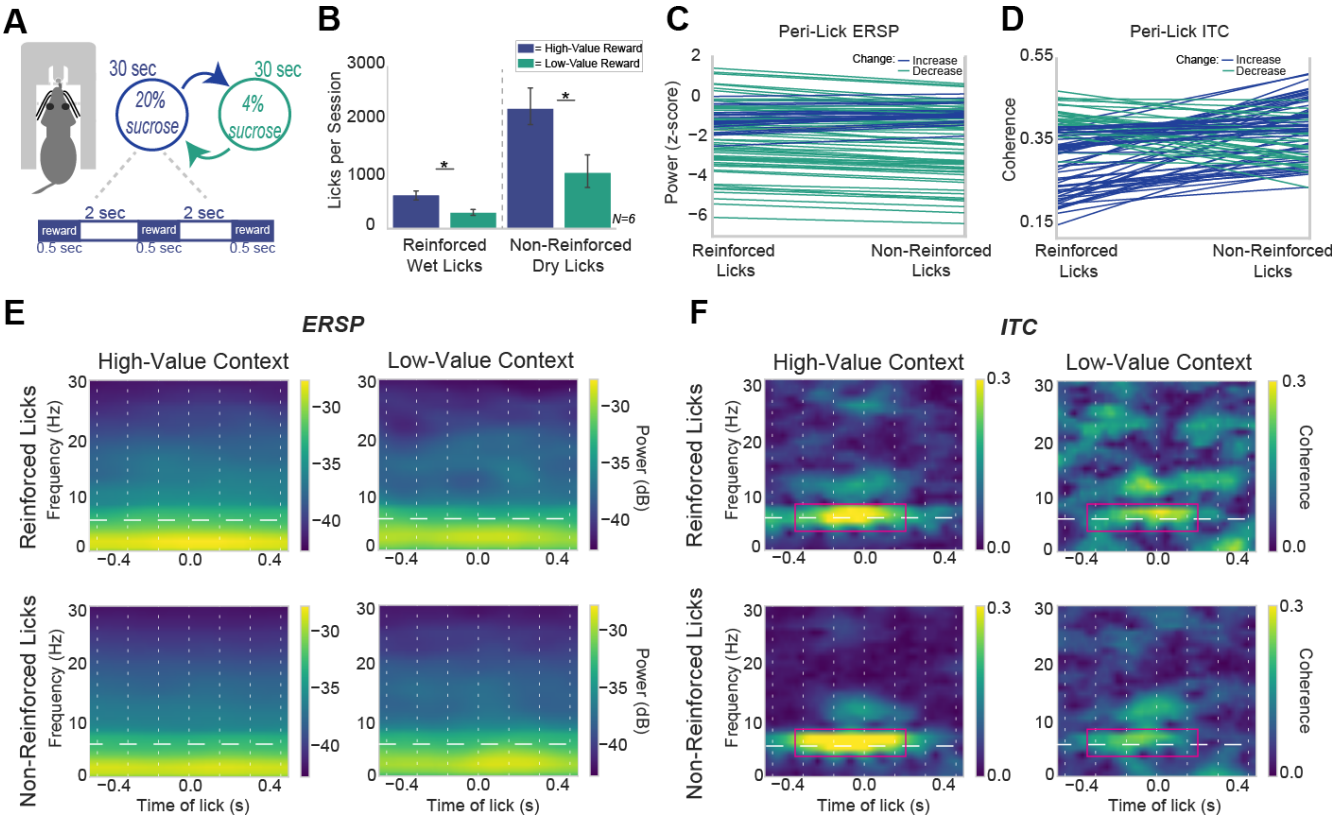

Figure 7: Reward context, not reinforcement per se, drives neuronal entrainment to the lick cycle. *A. The shifting values licking task was modified to include a 2 second period between pump activations. The 2 second "inter-pump interval" allows for non-reinforced licks (dry licks at the spout) to be recorded within the 30 second states of high or low value sucrose availability. B. Group summary of total licks (N=6 rats) showed that rats licked during the non-reinforced blocks and licked more in the higher-value blocks. Asterisk denotes p<0.05. C. Parallel line plots of maximum ERSP values for reinforced versus non-reinforced licks during the high-value blocks. Lines are colored by their direction (increase or decrease in power). There was no difference in power for reinforced versus non-reinforced licks (F(1,359)=2.52, p>0.05). D. Parallel line plots of maximum ITC values for reinforced versus non-reinforced licks during the high-value blocks. The majority of LFPs showed increased phase-locking to non-reinforced licks (blue lines), while electrodes from two rats show a slight decrease in phase-locking for non-reinforced licks (green lines). Overall group summaries show an increase in phase-locking for the non-reinforced licks (F(1,359) = 31.94, p<0.001). E,F. Example of time-frequency analysis of a LFP from a rat that showed decreased ERSP and ITC (magenta box) when the rat licked in the lower-value context. ITC was higher near the licking frequency when the higher value reward was available, regardless if the licks were reinforced or not. Horizontal white lines indicate the within-session licking frequencies and vertical white lines indicate the inter-lick intervals for each session.*

plots, shown in Figure 7F, revealed modest increases in phase-locking for the non-reinforced high-value licks, and minimal differences in the phase-locking for the reinforced versus non-

reinforced low-value context licks. These findings suggest that the reward context, rather than the properties of the delivered fluids, drives reward signaling in the rostral MFC.

Reward signaling depends on the medial frontal cortex

While the previous results implicate the MFC in lick-entrained rhythmic activity, specifically in encoding reward value, it was unclear of the specific role the MFC has in reward-based behaviors, or if the signals encoding reward value are due to or generated by other brain regions. We investigated if perturbing MFC activity would thus alter the encoding of relative reward value. Using the design described in Figure 1C, we recorded LFP activity from one hemisphere and infused muscimol, a GABA-A receptor agonist, into the opposite hemisphere via a drug cannula in four rats. Two of these rats had aligned electrode arrays and drug cannula (same cytoarchitectural area and layer). Two other rats were not precisely aligned, and electrophysiological data from those animals were not considered further. In all four rats, we did not observe any major behavioral change in the number of licks emitted during the muscimol sessions. (This is in contrast to our previous study with bilateral inactivations (Parent et al., 2015a), which clearly alter performance of the task.) The lack of behavioral effects of muscimol allowed us to assess potential electrophysiological changes without overt effects of the inactivations on the animals' licking behavior. There was a marginal decrease in the overall inter-lick intervals under muscimol (Wilcoxon rank-sum test, $p<0.05$), but no other effects of inactivation were apparent (e.g. duration of licking bouts).

In the two rats with aligned electrode arrays and drug cannulas, LFP activity during muscimol inactivations was dramatically altered. Muscimol infusions decreased the magnitude and rhythmicity of event-related potentials (ERP) during licking (Figure 8A), and decreased power (ERSP) during both high-value and low-value licks (Figure 8B, all electrodes plotted from two rats). This was confirmed in the spectral plots, shown from one example electrode from one rat (Figure 8D), where there is specifically a decrease in the low-frequency delta power. A repeated measures ANOVA on maximum ERSP values around the onset of licking revealed a

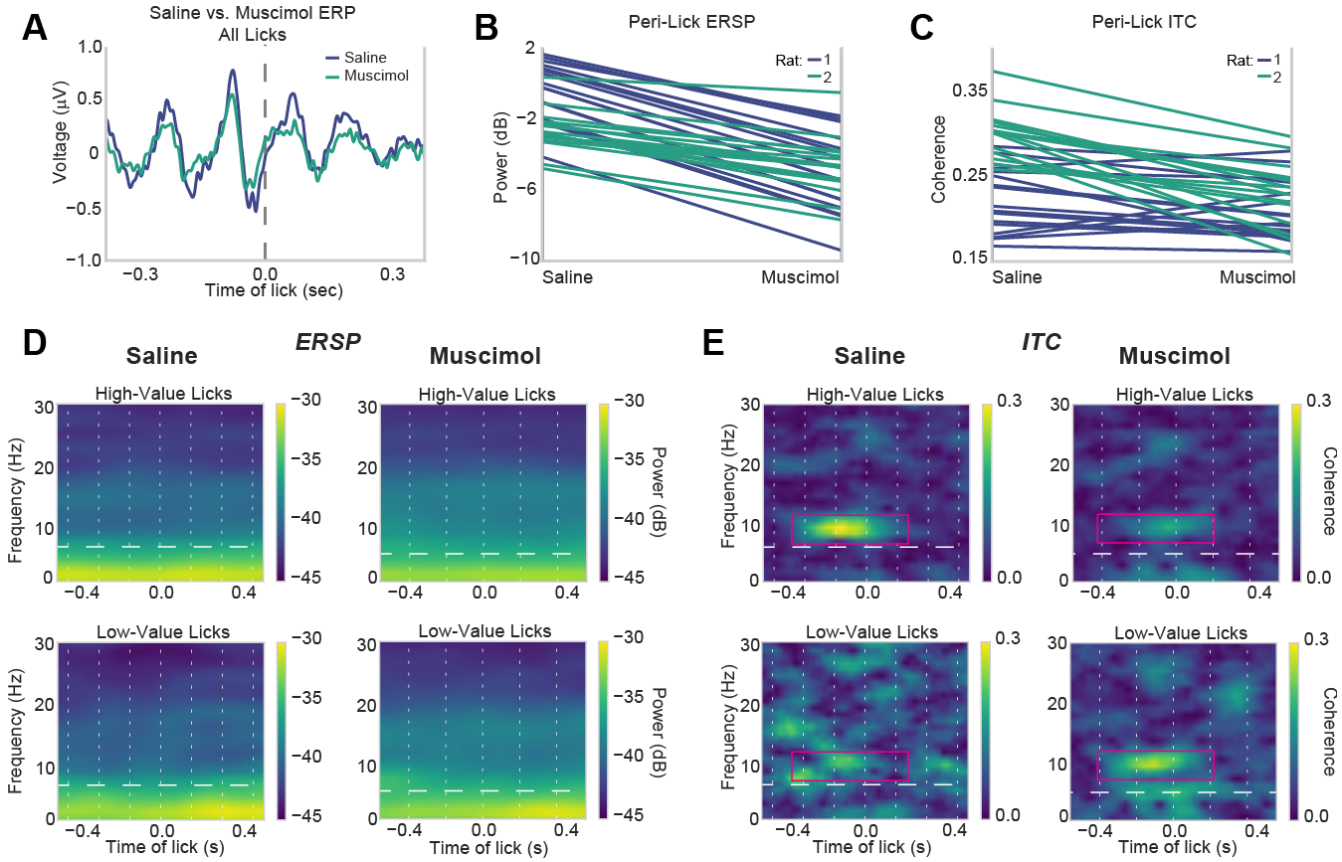

Figure 8: Reward signaling depends on neuronal activity in the MFC. *Rats were tested with an electrode array in the MFC in one hemisphere and an infusion cannula in the other hemisphere, and after infusions of either PBS or muscimol were made via the infusion cannula. A. Event-related potentials (ERP) from an electrode in the saline (blue line) and muscimol (yellow line) sessions. MFC inactivation had minor effects on the overall evoked signal in the MFC from the opposite hemisphere. B. However, parallel line plots revealed a decrease in power at the licking frequency (ERSP) at the onset of licking for the higher value fluid during the muscimol session compared to the saline session ($F(1,123) = 96.09$, $p<0.001$). C. Likewise, there was a reduction in phase entrainment (ITC) at the licking frequency for 28 of 32 electrodes ($F(1,123) = 18.17$, $p<0.001$). D,E. Example of time-frequency analysis of a LFP that showed reduced ERSP and ITC at the licking frequency (magenta box) in the muscimol test sessions. Effects were specific to licks for the high value reward. Horizontal white lines indicate the within-session licking frequencies and vertical white lines indicate the inter-lick intervals for each session. Note that muscimol in MFC slightly reduced the licking frequencies.*

decrease in power at lick-onset from saline to muscimol sessions ($F(1,123) = 96.09$, $p<0.001$).

Muscimol infusions also decreased the lick-entrained phase-locking in the theta frequency range. As seen in Figure 8C, 28 of 32 electrodes showed decreased phase-locking around the onset of licking. A repeated measures ANOVA revealed a significant difference in ITC

values for the saline and muscimol sessions ($F_{(1,123)}$ = 18.17, p<0.001). Spectral plots from an example electrode (Figure 8E) show diminished phase coherence in the theta frequency range for the high-value licks. The decrease in phase-locking therefore disrupted the previously evident differential signaling of reward value, suggesting that adequate reward signaling for relative rewards depends on the MFC.

Discussion

The goal of the present study was to investigate the neural representation of consummatory rewards in rat frontal cortex. We found lick-entrained neural activity of both local field potentials (Figure 1-3) and spikes (Figures 5-6) in the medial frontal cortex, specifically in the rostral prelimbic and medial agranular (AGm) regions. These signals developed with experience and encoded the relative reward value of the ingested liquid sucrose rewards (Figure 4). By modifying the behavioral task to include periods of non-reinforced licking, we found that this neuronal coding of relative value persisted beyond the period of reward delivery and suggest that it encodes the reward context (Figure 7). Finally, inactivation of the MFC diminished the encoding of reward value, establishing that the reward signals described in this study were generated, at least in part, by neurons in the MFC (Figure 8). Together, our results provide the first evidence that the rodent MFC tracks engagement in consummatory behavior and encodes the expected reward value of ingested foods and fluids.

Reward-related activity & encoding of relative reward value

Many previous studies have reported reward-related neural activity in the frontal cortex of humans (Glascher et al., 2009; Levy and Glimcher, 2011), primates (Watanabe, 1996; Roesch and Olson, 2004; Shidara and Richmond, 2002; Amiez et al., 2006; Padoa-Schiappa and Assad, 2006; Hayden et al., 2009; Luk and Wallis, 2009; Bouret and Richmond, 2010; Cai and Padoa-Schioppa, 2012), and rodents (Gutierrez et al., 2006; Petyko et al., 2009; Horst and Laubach, 2013; Petyko et al., 2015). However, all of these studies focused on the more medial and caudal

parts of the frontal cortex and did not assess reward signaling with respect to ongoing ingestive behavior. Our findings are the first to show that the most rostral area of MFC has a direct role in signaling the value of ingested foods and fluids, and does so in direct register with the animal's ongoing ingestive behavior. Activity from both LFPs and spikes in this region is entrained to the action of licking, and the two types of reward (high-value / high-concentration sucrose or low-value / low-concentration sucrose) are encoded differently by the extent of phase entrainment of the neuronal signals to the animal's lick cycle. Our findings also suggest that these MFC reward signals are generated by the taste of the liquid rewards, as the signals persist throughout blocks of time when licking is not reinforced and animals expect to receive relatively higher or lower value rewards (Figure 7). As such, the signals appear to reflect the reward context, representing the valued reward state that the animal is currently acting within. This idea is similar to previous concepts for prefrontal cortex which is involved in the "active maintenance" of behavior (Miller and Cohen, 2001) and represents the behavioral context (Hyman et al., 2012; Euston et al., 2012).

A role for MFC in the reward-guided control of orolingual behaviors?

Our studies (Figure 7) suggest that reward signals from the rostral MFC are driven by reward context, not by the taste properties of the liquid rewards, and these signals are phase-locked to licking behavior. As such, a major question is if this cortical region serves as a sort of "cingulate motor area" (Shima and Tanji, 1998) controlling voluntary orolingual movements based on the relative value of available rewards. Previous studies have investigated cortical regions within and near to the MFC and reported motor processing by these regions. Evidence has been reported for motor areas associated with the vibrissae (Brecht et al., 2004) and jaws/tongue (Adachi et al., 2008). These studies used intra-cortical microstimulation techniques and followed on classic studies on frontal motor maps by Hall and Lindholm (1974), Donoghue and Wise (1982), and Neafsey et al. (1986). Importantly, anatomical tract tracing studies between the AGm region of the MFC and a sensory representation of the perioral area, the trigeminal

355 mesencephalic nucleus or Vmes, reveal substantial projections from Vmes to AGm and prelimbic
356 cortex (Yoshida et al., 2009; Iida et al., 2010). The rostral agranular cortex projects to brainstem
357 nuclei controlling jaw-closing and jaw-opening (Haque et al., 2010). While there is not an easily
358 defined location in rat cortex for the jaw or tongue (like there is for the forelimb area, for
359 example), the available evidence suggests that the MFC contains an orofacial motor area. This
360 issue should be considered when interpreting results from studies of the rostral MFC of rodents.
361 Some studies have referred to the AGm area of MFC, in rat and mouse, as the secondary
362 motor cortex, or M2. A recent review by Barthas and Kwan (2017), and a commentary by Brecht
363 (2011), described how the "most medial and dorsal portion of the rodent frontal cortex" goes by
364 many names, such as AGm, M2, medial precentral cortex (PrCm), frontal orienting field (FOF),
365 dorsomedial prefrontal cortex (dmPFC), secondary frontal area (Fr2), and primary vibrissa motor
366 cortex (vM1). This brain region, while having some aspect of action or motor representations, is
367 not a true M1 in rodent, as AGm / M2 lesioned animals do not have overt motor deficits (Sul et
368 al., 2011). Regardless of the name, it is clear that this specific medial frontal area has a role in
369 adaptive choice behavior and reward signaling (Kargo et al., 2007; Sul et al., 2010; Sul et al.,
370 2011), specifically to map sensory input to motor actions. This interpretation applies to the
371 present study, which is unique in that it examined sensorimotor behavior specific to the
372 ingestive behavior of rats and found correlates of what might be a "premotor area" controlling
373 orolingual behavior and encoding expected values of ingested foods and fluids.
374 In the mouse literature, there is an area commonly referred to as the anterior lateral
375 motor cortex (ALM), which has been implicated in choice behavior during licking-related tasks
376 (Guo et al., 2014, Komiyama et al., 2010). Microstimulation of the ALM in mouse impairs licking
377 in mice, and the area also has involvement in preparatory activity and movement planning (Li et
378 al., 2015). While it is yet unclear if our recordings are from the rat version of ALM – some studies
379 have noted how ALM is distinct from M2 as ALM is traditionally a bit more lateral from M2
380 (Siniscalchi et al., 2016) – there are indeed similarities between published studies of ALM in the
381 mouse and our findings from the rostral MFC of the rat.

382 **Rhythmic encoding of relative reward value**

383 Two major frequencies that are prevalent in our findings are the 2-4 Hz delta rhythm and
384 4-8 Hz theta rhythm. To summarize our frequency-specific findings, we found a prominent delta-
385 range rhythm that occurred throughout the period when rats engaged in licking and was not
386 phase locked to the lick cycle and did not encode the relative value of the ingested fluids (Figure
387 3). A second rhythm occurred in the theta range (near the rats' licking frequency) that was
388 coupled to the rats' lick cycle (Figure 3). The theta-range signal showed significant phase tuning
389 at the onset of licking (Figures 1-3) and was enhanced when rats consumed the higher value
390 reward in our operant incentive contrast procedure (Figure 4). Spike activity was also coupled to
391 the lick cycle, although most prominently in the beta (10-30 Hz) and gamma (>30 Hz) ranges
392 (Figures 5-6), and all recordings of spike activity showed coherence with the licking frequency
393 content of the LFPs.

394 Unilateral reversible inactivations decreased theta phase tuning (Figure 8C,E) in the
395 opposite hemisphere, established that these signals depended on neurons within the MFC. It is
396 important to note that these inactivations were unilateral and there were no overt behavioral
397 changes to the animals' licking behavior during inactivations. This is in strong contrast to
398 bilateral inactivations of the same cortical area which leads to temporally fragmented licking
399 and a failure of rats to follow learned strategies to maximize reward consumption (Parent et al.,
400 2015a). It is not uncommon for unilateral cross-hemispheric inactivations to show less dramatic
401 effects on behavior (Ambroggi et al., 2008), and it was necessary for our interpretations to have
402 the rats maintain their behavior without normal MFC function. Our findings from the
403 inactivation study bolster evidence for the role of MFC in encoding reward value and suggest
404 that adequate signaling of reward value depends on local activity within the rostral MFC.

405 Theta rhythms are a prominent feature within the frontal cortex. Many studies have
406 reported theta rhythmic activity that represents many different aspects of behavior, such as
407 interval timing (Parker et al., 2014; Emmons et al., 2016), cognitive control (Cavanaugh and
408 Frank, 2014), errors and adaptive control (Narayanan et al., 2013; Laubach et al., 2015), freezing

behaviors related to fear-conditioning (Karalis et al., 2016), and consummatory reward-related behavior (Horst and Laubach, 2013). The prominence of the theta rhythm in rodent frontal cortex in consummatory and reward-related studies is especially interesting because rats naturally lick within the 6-8 Hz theta range (Weijnen, 1998) and open/close their jaw in the 5-7 Hz range (Sasamoto et al., 1990). These behaviors are driven by a brainstem central pattern generator (CPG) for mastication and licking (Travers et al., 1997). However, it is not solely licking that occurs in a low-frequency rhythmic manner: many other orofacial behaviors such as chewing / mastication (Nakamura and Katakura, 1995), breathing, sniffing and whisking (Moore et al., 2013) occur in a rhythmic manner as well. These orofacial motor behaviors are controlled by CPGs in the brainstem (Moore et al., 2014), which receive projections from the rostral MFC (Yoshida et al., 2009; Haque et al., 2010; Iida et al., 2010).

Conclusion

We have shown a role for the rostral area of the rat medial frontal cortex in encoding the value of consummatory rewards in a rhythmic manner. These signals may have a key role in terminating monitoring processes associated with adaptive control (Narayanan et al., 2013; Bekolay et al., 2014), signaling outcomes during foraging behavior (Caracheo et al., 2013), and in implementing the use of learned strategies to maximize reward consumption (Parent et al., 2015a). Our study provides support for an emerging concept that the MFC contains neurons that are directly modulated by the act of consuming a reward (Petyko et al., 2009; Bouret and Richmond, 2010; Horst and Laubach, 2012; Horst and Laubach, 2013; Petyko et al., 2015). If integrated with gustatory information, which has recently been shown to be encoded by mPFC neurons (Jezzini et al., 2013), the MFC reward signals described in our study could enable control over food-based decisions and self control over eating. These issues have clinical implications given the association of the MFC with loss of control in obesity (Volkow et al., 2011) and eating disorders such as anorexia (Uher et al., 2004).

Methods

All procedures carried out in this set of experiments were approved by the Animal Use and Care Committees at the John B. Pierce Laboratory (where some of the experiments were conducted) and American University. All procedures conformed to the standards of the National Institutes of Health Guide for the Care and Use of Laboratory Animals. All efforts were taken to minimize the number of animals used and to reduce pain and suffering.

Animals.

Male Long Evans rats weighing between 300 and 325 g were purchased from Harlan or Charles River. Rats were given one week to acclimate with daily handling prior to behavioral training or surgery and were then kept with regulated access to food to maintain 90% of their free-freeding body weight. They were given ~18g of standard rat chow each day in the evenings following experiments. Rats were single-housed in their home cages in a 12h light/dark cycle colony room, with experiments occurring during the light cycle. A total of 11 rats had a microwire array implanted into medial frontal cortex. Some rats additionally had a drug cannula implanted into the opposite hemisphere using the same stereotaxic coordinates. Arrays were made by Tucker-Davis Technologies and consisted of 16 blunt-cut 50-μm tungsten wires, insulated with Formvar, separated by 250 μm within each row and 500 μm between rows. In vitro impedances for the microwires were ~150 kΩ.

Surgeries.

Animals had full access to food and water in the days prior to surgery. Stereotaxic surgery was performed using standard methods (e.g., Narayanan and Laubach, 2006). Briefly, animals were lightly anesthetized with isoflurane (2.5% for ~2 minutes), and were then injected intraperitoneally with ketamine (100mg/kg) and either xylazine (10 mg/kg) or dexdomitor (0.25mg/kg) to maintain a surgical plane of anesthesia. Craniotomies were made above the implant location. Microwire arrays were placed into the medial frontal cortex (coordinates from

bregma: AP: +3.2 mm; ML: ± 1.0 mm; DV: -2.2 mm from the surface of the brain, at a 12° posterior angle). Four skull screws were placed along the edges of the skull and a ground wire was secured in the intracranial space above the posterior cerebral cortex. Electrode arrays were connected to a headstage cable and modified Plexon preamplifier during surgery and recordings were made to assess neural activity during array placement. Drug cannulas, 26-gauge PEEK (Plastics One), were implanted prior to the microwire arrays using similar procedures. Craniotomies were sealed using cyanocrylate (Slo-Zap) and an accelerator (Zip Kicker), and methyl methacrylate dental cement (AM Systems) was applied and affixed to the skull via the skull screws. Animals were given a reversal agent for either xylazine (yohimbine, 2mg/ml) or dexdomitor (Antisedan, s.c. 0.25 mg/ml) and Carprofen (5 mg/kg, s.c.) was administered for postoperative analgesia. Animals recovered from surgery in their home cages for at least one week with full food and water, and were weighed and monitored each day following surgery.

Behavioral Tasks.

Behavioral Apparatus.

Rats were trained in operant chambers housed within a sound-attenuating external chamber (Med Associates, St. Albans, VT). Operant chambers contained a custom-made drinking spout that was connected to multiple fluid lines allowing for multiple fluids to be consumed at the same location. The spout was centered on one side of the operant chamber wall at a height of 5 to 6.5cm from the chamber floor. Tygon tubing connected to the back of the drinking spout would administer the fluid from a 60cc syringe hooked up to a PHM-100 pump (Med Associates). A “light-pipe” lickometer (Med Associates) detected licks via an LED photobeam, and each lick triggered the pump to deliver roughly 0.025 ml per 0.5 second. Behavioral protocols were run though Med-PC version IV (Med Associates), and behavioral data was sent via TTL pulses from the Med-PC software to the Plexon recording system.

Continuous-Access Shifting Values Licking Task

The operant licking task used here is similar to that previously described in Parent et al. (2015a,b). Briefly, rats were placed in the operant chamber for thirty minutes, where they were solely required to lick at the drinking spout to obtain a liquid sucrose reward. Licks activated the syringe pumps to deliver liquid sucrose over 0.5 second. Every 30 seconds, the reward alternated between a high concentration (20% weight per volume) and low concentration (2-4% wt/vol) of sucrose. The animal's licking behavior was constantly monitored throughout the test sessions.

Instrumental Shifting Values Licking Task

The operant licking task used above was modified slightly to allow for assessment of reinforced versus non-reinforced licks. A 2 second inter-pump interval was included between each pump activation. In other words, the rat would lick to activate a liquid sucrose reward for 0.5 sec, and then once the pump stopped delivering fluid, no reward was delivered again for 2 sec. The next lick after the 2 sec interval would initiate the next pump activation. Licks during the 2 sec inter-trial period were *instrumental*.

Electrophysiological Recordings.

Multi-electrode Recordings.

Electrophysiological recordings were made using a Plexon Multichannel Acquisition Processor (MAP; Plexon; Dallas, TX). Local field potentials were sampled on all electrodes and recorded continuously throughout the behavioral testing sessions using the Plexon system via National Instruments A/D card (PCI-DIO-32HS). The sampling rate was 1 kHz. The head-stage filters (Plexon) were at 0.5 Hz and 5.9 kHz. Electrodes with unstable signals or prominent peaks at 60 Hz in plots of power spectral density were excluded from quantitative analysis.

Paired recordings with Muscimol infusion

Animals were tested with muscimol infusions in one hemisphere and recordings of neural activity in the opposite hemisphere. For control sessions, phosphate-buffered saline (PBS) was infused into MFC. The next day, muscimol (Sigma-Aldrich, St Louis, MO) was infused at 0.1 µg/µl. Infusions were performed by inserting a 33-gauge injector into the guide cannula, and 1.0 µl of fluid was delivered at a rate of 15 µl per h (0.25 µl per min) with a syringe infusion pump (KDS Scientific, Holliston, MA). The injector was connected to a 10 µl Hamilton syringe via 0.38 mm diameter polyethylene tubing. After infusion was finished, the injector was left in place for at least 4 minutes to allow for diffusion of the fluid. The injector was slowly removed and the headstage cable was subsequently plugged into the animal's implant. Rats were tested in the instrumental shifting values licking task 1 hour after the PBS or muscimol infusions. Recordings were made the day following the infusion session without any manipulation to verify recovery from the inactivation session.

Histology.

After all experiments were completed, rats were deeply anesthetized via an intraperitoneal injection of Euthasol (100mg/kg) and then transcardially perfused using 4% paraformaldehyde in phosphate-buffered saline. Brains were cryoprotected with a 20% sucrose and 10% glycerol mixture and then sectioned horizontally on a freezing microtome. The slices were mounted on gelatin-subbed slides and stained for Nissl substance with thionin.

Data Analysis.

Software

All data were analyzed using GNU Octave (https://www.gnu.org/software/octave/), Python (Anaconda distribution: https://www.continuum.io/), and R (https://www.r-project.org/). Analyses were run as Jupyter notebooks (http://jupyter.org/). Computer code used in this study is available upon request from the corresponding author.

Statistical Analysis

Statistical testing was performed in R. Paired t-tests were used throughout the study and repeated-measures ANOVA (with the error term due to subject) were used to compare data across training sessions (Figure 4), reinforced versus non-reinforced licks (Figure 7), and PBS versus muscimol (Figure 8).

Data Analysis: Local Field Potentials

Electrophysiological data were first briefly assessed in NeuroExplorer (http://www.neuroexplorer.com/). Subsequent processing was done using signal processing routines in GNU Octave. Analysis of Local Field Potentials (LFP) was carried out using the EEGLab toolbox (http://sccn.ucsd.edu/eeglab/) (Event-Related Spectral Power and Inter-Trial Coherence) and Neurospec 2.0 (http://www.neurospec.org/) (spike-lick and spike-field coherence). Circular statistics were calculated using the *circular* library for R. Graphical plots of data were made using the *matplotlib* and *seaborn* library for Python. Analyses were typically conducted in Jupyter notebooks, and interactions between Python, R, and Octave were implemented using the *rpy2* and *oct2py* libraries for Python.

To measure the amplitude and phase of LFP in the frequency range of licking, LFPs were bandpass-filtered using eeglab's *eegfilt* function, with a fir1 filter (Widmann & Schröger, 2012), centered at the rat's licking frequency (licking frequency $\pm$ inter-quartile range; typically around 4 to 9 Hz), and were subsequently z-scored. Analyses were performed with a pre/post window of 2 seconds, and the Hilbert transform was used to obtain the amplitude and phase of the LFP.

To measure the consistency of LFP phase, 500 licks were randomly chosen from one session from each rat along with 500 random time points that were chosen based on shuffling the inter-lick intervals from all licks in the rat's session. After creating peri-event matrices from filtered and z-scored LFP data, the Hilbert transform was applied to obtain the phase angle and amplitude for each electrode, and the phase angles were converted to circular data using the *circular* library for R (Agostinelli and Lund, 2013), and were then used in the function *rho.circular*

to obtain mean resultant vector length, and *mean.circular* to obtain the actual phase angle. The *rao.spacing.test* function from R's circular library was used to obtain the test statistic and corresponding p-value that tells if the phase angles at the onset of licking pointed in a specific direction or were uniformly distributed (between 0° and 360°).

For inter-trial phase coherence (ITC) and event-related spectral power (ERSP) spectral analyses, LFP data was preprocessed using eeglab's *eegfilt* function with a fir1 filter and was bandpass filtered from 0 to 100 Hz. For group summaries, ITC and ERSP matrices were z-scored for that given rat after bandpass filtering the data. Peri-lick matrices were then formed by using a pre/post window of 2 seconds on each side, and the *newtimef* function from the eeglab toolbox was used to generate the time-frequency matrices for ITC and ERSP up to 30 Hz. Group summaries for ITC and ERSP were performed by obtaining the maximum ITC value within a time window of ±2 interlick intervals (typically ~±375 milliseconds) around licking, and obtaining the maximum ERSP value within that same window. Each electrode's maximum ITC and ERSP value for each type of lick (high-value or low-value lick) were used in the ANOVAs for group summaries. Finally, a "value index" was calculated to assess differences in ITC and ERSP measures associated with consumption of the higher and lower value rewards. The index was defined by the difference between the measures divided by the measure for the higher value condition, e.g. $(ITC_{Hi} - ITC_{Lo})/ITC_{Hi}$.

Shuffling methods were used to compare ERSP and ITC values for observed and shuffled licks (obtained by calculating inter-lick intervals, shuffling their trial order, and adding the intervals to the first lick in each behavioral session). This gave a set of surrogate licks with random timing unrelated to the animal's behavior. Subsets of 50 licks and shuffled events were randomly chosen from each behavioral session and ERSP and ITC statistics were calculated for the subsets of observed and shuffled data.

Data Analysis: Spike Activity

Exploratory analysis of on-line identified single units showed spike probabilities below 0.1

583 for all single units recorded in the task. Therefore, we used multi-unit activity (MUA) to relate
584 spike activity to the animals' lick cycles and related LFP signals. MUA was identified using the
585 Plexon Offline Sorter v. 4.3 (Plexon, Dallas, TX). All recorded spike waveforms were thresholded
586 (±2.7 times the standard deviation for the collection of waveforms) and "automatic artifact
587 invalidation" was applied. Then, using routines in NeuroExplorer v. 5 (Nex Technologies,
588 Madison, AL), we measured spike probabilities for all recorded MUAs around the higher and
589 lower values licks, using 0.001 sec bins. Spike probabilities were compared for the two lick
590 values using a paired t-test (in R). To measure Spike-Lick Coherence (SLC), we used routines
591 (sp2_m1.m) from Neurospec 2.0 (*http://www.neurospec.org/*). The following parameters were
592 used: Segment power = 12 (4096 points, frequency resolution: 0.244 Hz) and Hanning filtering
593 with 50% tapering. To measure Spike-Field Coherence (SFC), we also used routines (sp2a_m)
594 from Neurospec 2.0, and analyzed bandpass filtered LFP (processed as described above; licking
595 frequency $\pm$ inter-quartile range) and the following parameters: Segment power = 10 (1024
596 points, frequency resolution: 0.977 Hz), Hanning filtering with 50% tapering, and line noise
597 removal for the LFPs at 60 Hz.

References

Adachi, K., Murray, G. M., Lee, J.-C., & Sessle, B. J. (2008). Noxious Lingual Stimulation Influences the Excitability of the Face Primary Motor Cerebral Cortex (Face MI) in the Rat. *Journal of Neurophysiology*, *100*(3), 1234–1244.

Agostinelli, C., & Lund, U. (2013). R package 'circular': Circular Statistics (version 0.4-7). URL https://r-forge.r-project.org/projects/circular/

Ambroggi, F., Ishikawa, A., Fields, H. L., & Nicola, S. M. (2008). Basolateral Amygdala Neurons Facilitate Reward-Seeking Behavior by Exciting Nucleus Accumbens Neurons. *Neuron*, *59*(4), 648–661.

Amiez, C., Joseph, J. P., & Procyk, E. (2005). Reward Encoding in the Monkey Anterior Cingulate Cortex. *Cerebral Cortex*, *16*(7), 1040–1055.

Barthas, F., & Kwan, A. C. (2017). Secondary Motor Cortex: Where “Sensory” Meets “Motor” in the Rodent Frontal Cortex. *Trends in Neurosciences*, *40*(3), 181–193.

Bekolay, T., Laubach, M. & Eliasmith, C. (2014) A Spiking Neural Integrator Model of the Adaptive Control of Action by the Medial Prefrontal Cortex. *Journal of Neuroscience* 34, 1892–1902.

Bouret, S., & Richmond, B. J. (2010). Ventromedial and Orbital Prefrontal Neurons Differentially Encode Internally and Externally Driven Motivational Values in Monkeys. *Journal of Neuroscience*, *30*(25), 8591–8601.

Brecht, M. (2011). Movement, Confusion, and Orienting in Frontal Cortices. *Neuron*, *72*(2), 193–196.

Brecht, M., Krauss, A., Muhammad, S., Sinai-Esfahani, L., Bellanca, S., & Margrie, T. W. (2004). Organization of rat vibrissa motor cortex and adjacent areas according to cytoarchitectonics, microstimulation, and intracellular stimulation of identified cells. *The Journal of Comparative Neurology*, *479*(4), 360–373.

Cai, X., & Padoa-Schioppa, C. (2012). Neuronal Encoding of Subjective Value in Dorsal and Ventral Anterior Cingulate Cortex. *Journal of Neuroscience*, *32*(11), 3791–3808.

Caracheo, B. F., Emberly, E., Hadizadeh, S., Hyman, J. M., & Seamans, J. K. (2013). Abrupt changes in the patterns and complexity of anterior cingulate cortex activity when food is introduced into an environment. Frontiers in neuroscience, 7, 74.

Carracedo, L. M., Kjeldsen, H., Cunnington, L., Jenkins, A., Schofield, I., Cunningham, M. O., Whittington, M. A. (2013). A Neocortical Delta Rhythm Facilitates Reciprocal Interlaminar Interactions via Nested Theta Rhythms. *Journal of Neuroscience*, *33*(26), 10750–10761.

Cavanagh, J. F., & Frank, M. J. (2014). Frontal theta as a mechanism for cognitive control. *Trends in Cognitive Sciences*, *18*(8), 414–421.

Donnelly, N. A. *et al.* Oscillatory Activity in the Medial Prefrontal Cortex and Nucleus Accumbens Correlates with Impulsivity and Reward Outcome. *PLoS ONE* 9, e111300 (2014).

Donoghue, J. P., & Wise, S. P. (1982). The motor cortex of the rat: cytoarchitecture and

635 microstimulation mapping. *Journal of Comparative Neurology*, *212*(1), 76–88.
636 Emmons, E. B., Ruggiero, R. N., Kelley, R. M., Parker, K. L., & Narayanan, N. S. (2016).
637 Corticostriatal Field Potentials Are Modulated at Delta and Theta Frequencies during
638 Interval-Timing Task in Rodents. *Frontiers in Psychology*, *7*.
639 Erlich, J. C., Bialek, M. & Brody, C. D. A Cortical Substrate for Memory-Guided Orienting in the
640 Rat. *Neuron* 72, 330–343 (2011).
641 Euston, D. R., Gruber, A. J., & McNaughton, B. L. (2012). The Role of Medial Prefrontal Cortex in
642 Memory and Decision Making. *Neuron*, *76*(6), 1057–1070.
643 Floyd, N. S., Price, J. L., Ferry, A. T., Keay, K. A., & Bandler, R. (2000). Orbitomedial prefrontal
644 cortical projections to distinct longitudinal columns of the periaqueductal gray in the rat.
645 *Journal of Comparative Neurology*, *422*(4), 556–578.
646 Floyd, N. S., Price, J. L., Ferry, A. T., Keay, K. A., & Bandler, R. (2001). Orbitomedial prefrontal
647 cortical projections to hypothalamus in the rat. *Journal of Comparative Neurology*, *432*(3),
648 307–328.
649 Gabbott, P. L. ., Warner, T. A., Jays, P. R. ., & Bacon, S. J. (2003). Areal and synaptic
650 interconnectivity of prelimbic (area 32), infralimbic (area 25) and insular cortices in the
651 rat. *Brain Research*, *993*(1–2), 59–71.
652 Gabbott, P. L. A., Warner, T. A., Jays, P. R. L., Salway, P., & Busby, S. J. (2005). Prefrontal cortex in
653 the rat: Projections to subcortical autonomic, motor, and limbic centers. *The Journal of*
654 *Comparative Neurology*, *492*(2), 145–177.
655 Glascher, J., Hampton, A. N., & O'Doherty, J. P. (2009). Determining a Role for Ventromedial
656 Prefrontal Cortex in Encoding Action-Based Value Signals During Reward-Related
657 Decision Making. *Cerebral Cortex*, *19*(2), 483–495.
658 Guo, Z. V., Li, N., Huber, D., Ophir, E., Gutnisky, D., Ting, J. T., … Svoboda, K. (2014). Flow of
659 Cortical Activity Underlying a Tactile Decision in Mice. *Neuron*, *81*(1), 179–194.
660 Gutierrez, R. Orbitofrontal Ensemble Activity Monitors Licking and Distinguishes Among Natural
661 Rewards. *Journal of Neurophysiology* 95, 119–133 (2006).
662 Hall, R. D., & Lindholm, E. P. (1974). Organization of Motor and Somatosensory neocortex in the
663 albino rat. *Brain Research*, *66*, 23–38.
664 Haque, T., Yamamoto, S., Masuda, Y., Kato, T., Sato, F., Uchino, K., … Yoshida, A. (2010). Thalamic
665 afferent and efferent connectivity to cerebral cortical areas with direct projections to
666 identified subgroups of trigeminal premotoneurons in the rat. *Brain Research*, *1346*, 69–
667 82.
668 Hassan, S. F., Cornish, J. L. & Goodchild, A. K. Respiratory, metabolic and cardiac functions are
669 altered by disinhibition of subregions of the medial prefrontal cortex: The prefrontal
670 cortex and autonomic functions. *The Journal of Physiology* 591, 6069–6088 (2013).
671 Hayden, B. Y., Pearson, J. M., & Platt, M. L. (2009). Fictive reward signals in the anterior cingulate

cortex. *Science*, *324*(5929), 948–950.

Horst, N.K, & Laubach, M. (2012) Working with memory: evidence for a role for the medial prefrontal cortex in performance monitoring during spatial delayed alternation. *Journal of Neurophysiology*, 108(12), 3276-88.

Horst, N. K., & Laubach, M. (2013). Reward-related activity in the medial prefrontal cortex is driven by consumption. *Frontiers in Neuroscience*, *7*(56).

Hyman, J.M, Ma, L., Balaguer-Ballester, E., Durstewitz, D., Seamans, J.K. (2012).Contextual encoding by ensembles of medial prefrontal cortex neurons. *Proceedings of the National Academy of Sciences*, *109*(13), 5086-5091.

Iida, C., Oka, A., Moritani, M., Kato, T., Haque, T., Sato, F., … Yoshida, A. (2010). Corticofugal direct projections to primary afferent neurons in the trigeminal mesencephalic nucleus of rats. *Neuroscience*, *169*(4), 1739–1757.

Ito, S., Stuphorn, V., Brown, J. W., & Schall, J. D. (2003). Performance monitoring by the anterior cingulate cortex during saccade countermanding. *Science*, *302*(5642), 120-122.

Jezzini, A., Mazzucato, L., La Camera, G. & Fontanini, A. Processing of Hedonic and Chemosensory Features of Taste in Medial Prefrontal and Insular Networks. *Journal of Neuroscience* 33, 18966–18978 (2013).

Karalis, N., Dejean, C., Chaudun, F., Khoder, S., Rozeske, R. R., Wurtz, H., … Herry, C. (2016). 4-Hz oscillations synchronize prefrontal–amygdala circuits during fear behavior. *Nature Neuroscience*, *19*(4), 605–612.

Kargo, W. J., Szatmary, B., & Nitz, D. A. (2007). Adaptation of Prefrontal Cortical Firing Patterns and Their Fidelity to Changes in Action-Reward Contingencies. *Journal of Neuroscience*, *27*(13), 3548–3559.

Komiyama, T., Sato, T. R., O'Connor, D. H., Zhang, Y.-X., Huber, D., Hooks, B. M., … Svoboda, K. (2010). Learning-related fine-scale specificity imaged in motor cortex circuits of behaving mice. *Nature*, *464*(7292), 1182–1186.

Laubach, M., Caetano, M. S., & Narayanan, N. S. (2015). Mistakes were made: Neural mechanisms for the adaptive control of action initiation by the medial prefrontal cortex. *Journal of Physiology-Paris*, *109*(1–3), 104–117.

Levy, D. J., & Glimcher, P. W. (2011). Comparing Apples and Oranges: Using Reward-Specific and Reward-General Subjective Value Representation in the Brain. *Journal of Neuroscience*, *31*(41), 14693–14707.

Li, N., Chen, T.-W., Guo, Z. V., Gerfen, C. R., & Svoboda, K. (2015). A motor cortex circuit for motor planning and movement. *Nature*, *519*(7541), 51–56.

Luk, C.-H., & Wallis, J. D. (2009). Dynamic Encoding of Responses and Outcomes by Neurons in Medial Prefrontal Cortex. *Journal of Neuroscience*, *29*(23), 7526–7539.

Miller, E. K., & Cohen, J. D. (2001). An integrative theory of prefrontal cortex function. *Annual*

Review of Neuroscience, *24*(1), 167–202.

Moore, J. D., Deschênes, M., Furuta, T., Huber, D., Smear, M. C., Demers, M., & Kleinfeld, D. (2013). Hierarchy of orofacial rhythms revealed through whisking and breathing. Nature, 497(7448), 205-210.

Moore, J. D., Kleinfeld, D., & Wang, F. (2014). How the brainstem controls orofacial behaviors comprised of rhythmic actions. *Trends in Neurosciences*, *37*(7), 370–380.

Nakamura, Y., & Katakura, N. (1995). Generation of masticatory rhythm in the brainstem. *Neuroscience Research*, *23*, 1–19.

Narayanan, N. S., & Laubach, M. (2006). Top-down control of motor cortex ensembles by dorsomedial prefrontal cortex. *Neuron*, *52*(5), 921-931.

Narayanan, N. S., Cavanagh, J. F., Frank, M. J., & Laubach, M. (2013). Common medial frontal mechanisms of adaptive control in humans and rodents. *Nature Neuroscience*, *16*(12), 1888–1895.

Neafsey, E. J., Bold, E. L., Haas, G., Hurley-Gius, K. M., Quirk, G., Sievert, C. F., & Terreberry, R. R. (1986). The Organization of the Rat Motor Cortex: A Microstimulation Mapping Study. *Brain Research Reviews*, *11*, 77–96.

Otis, J. M., Namboodiri, V. M. K., Matan, A. M., Voets, E. S., Mohorn, E. P., Kosyk, O., … Stuber, G. D. (2017). Prefrontal cortex output circuits guide reward seeking through divergent cue encoding. *Nature*, *543*(7643), 103–107.

Padoa-Schioppa, C., & Assad, J. A. (2006). Neurons in the orbitofrontal cortex encode economic value. *Nature*, *441*(7090), 223–226.

Paxinos G and Watson C (1997). Paxinos and Watson's The Rat Brain in Stereotaxic Coordinates, Third Edition. Elsevier Academic Press, San Diego.

Parent, M. A., Amarante, L. M., Liu, B., Weikum, D., & Laubach, M. (2015a). The medial prefrontal cortex is crucial for the maintenance of persistent licking and the expression of incentive contrast. *Frontiers in Integrative Neuroscience*, *9*.

Parent, M. A., Amarante, L. M., Swanson, K., & Laubach, M. (2015b). Cholinergic and ghrelinergic receptors and KCNQ channels in the medial PFC regulate the expression of palatability. *Frontiers in Behavioral Neuroscience*, *9*.

Parker, K. L., Chen, K.-H., Kingyon, J. R., Cavanagh, J. F., & Narayanan, N. S. (2014). D1-Dependent 4 Hz Oscillations and Ramping Activity in Rodent Medial Frontal Cortex during Interval Timing. *Journal of Neuroscience*, *34*(50), 16774–16783.

Petykó, Z., Tóth, A., Szabó, I., Gálosi, R., & Lénárd, L. (2009). Neuronal activity in rat medial prefrontal cortex during sucrose solution intake: *NeuroReport*, *20*(14), 1235–1239.

Petykó, Z., Gálosi, R., Tóth, A., Máté, K., Szabó, I., Szabó, I., … Lénárd, L. (2015). Responses of rat medial prefrontal cortical neurons to Pavlovian conditioned stimuli and to delivery of appetitive reward. *Behavioural Brain Research*, *287*, 109–119.

Reppucci, C. J. & Petrovich, G. D. Organization of connections between the amygdala, medial prefrontal cortex, and lateral hypothalamus: a single and double retrograde tracing study in rats. *Brain Structure and Function* 221, 2937–2962 (2016).

Roesch, M., & Olson, C. (2004). Neuronal Activity Related to Reward Value and Motivation in Primate Frontal Cortex. *Science*, *304*(5668), 307–310.

Sasamoto, K., Zhang, G., & Iwasaki, M. (1990). Two types of rhythmical jaw movements evoked by stimulation of the rat cortex. *Japanese Journal of Oral Biology*, *32*(1), 57–68.

Shidara, M. & Richmond, B. J. Anterior Cingulate: Single Neuronal Signals Related to Degree of Reward Expectancy. *Science* 296, 1709–1711 (2002).

Shima, K. & Tanji, J. Role for cingulate motor area cells in voluntary movement selection based on reward. *Science* 282, 1335–1338 (1998).

Siniscalchi, M. J., Phoumthipphavong, V., Ali, F., Lozano, M., & Kwan, A. C. (2016). Fast and slow transitions in frontal ensemble activity during flexible sensorimotor behavior. *Nature Neuroscience*, *19*(9), 1234–1242.

Stapleton, J. R., Lavine, M. L., Wolpert, R. L., Nicolelis, M. A., & Simon, S. A. (2006). Rapid taste responses in the gustatory cortex during licking. Journal of Neuroscience, 26(15), 4126-4138.

Sul, J. H., Kim, H., Huh, N., Lee, D., & Jung, M. W. (2010). Distinct Roles of Rodent Orbitofrontal and Medial Prefrontal Cortex in Decision Making. *Neuron*, *66*(3), 449–460.

Sul, J. H., Jo, S., Lee, D., & Jung, M. W. (2011). Role of rodent secondary motor cortex in value-based action selection. *Nature Neuroscience*, *14*(9), 1202–1208.

Travers, J. B., Dinardo, L. A., & Karimnamazi, H. (1997). Motor and premotor mechanisms of licking. *Neuroscience & Biobehavioral Reviews*, *21*(5), 631–647.

Uher, R., Murphy, T., Brammer, M. J., Dalgleish, T., Phillips, M. L., Ng, V. W., ... & Treasure, J. (2004). Medial prefrontal cortex activity associated with symptom provocation in eating disorders. *American Journal of Psychiatry*, *161*(7), 1238-1246.

Volkow, N. D., Wang, G. J., & Baler, R. D. (2011). Reward, dopamine and the control of food intake: implications for obesity. *Trends in cognitive sciences*, *15*(1), 37-46.

Watanabe, M. (1996). Reward expectancy in primate prefrontal neurons. *Nature*, *382*((6592), 629).

Widmann, A., & Schröger, E. (2012) Filter effects and filter artifacts in the analysis of electrophysiological data. *Frontiers in Psychology*, 3:233.

Weijnen, J. A. (1998). Licking behavior in the rat: measurement and situational control of licking frequency. *Neuroscience & Biobehavioral Reviews*, *22*(6), 751–760.

Yoshida, A., Taki, I., Chang, Z., Iida, C., Haque, T., Tomita, A., ... Shigenaga, Y. (2009). Corticofugal projections to trigeminal motoneurons innervating antagonistic jaw muscles in rats as demonstrated by anterograde and retrograde tract tracing. *The Journal of Comparative Neurology*, *514*(4), 368–386.